ISTITUTO NAZIONALE DI FISICA NUCLEARE
Laboratori Nazionali di Frascati

LNF-87/2(P)
21 Gennaio 1987

A.Bianconi, I.Davoli, S.Della Longa, J.Garcia, K.B.Garg, A. Kotani, and A. Marcelli:

THE INTERATOMIC INTERMEDIATE VALENCE STATE OF INSULATING CORRELATED OXIDES CeO_2, PrO_2 AND TbO_2

Invited talk given at the Inter. Conf. on "Valence Fluctuations" Bangalore India, (January 4-9 1987)

Servizio Documentazione
dei Laboratori Nazionali di Frascati
Cas. Postale 13 - Frascati (Roma)

INFN - Laboratori Nazionali di Frascati
Servizio Documentazione

LNF-87/2(P)
21 Gennaio 1987

THE INTERATOMIC INTERMEDIATE VALENCE STATE OF INSULATING CORRELATED OXIDES CeO_2, PrO_2 AND TbO_2

A. Bianconi°, I. Davoli@, S. Della Longa°, J. Garcia°•, K. B. Garg°*, A. Kotani§, A. Marcelli#

°Dipartimento di Fisica, Università di Roma La Sapienza, 00185 Roma, Italy
#Laboratori Nazionali di Frascati-INFN, P.O. Box 13, 00044 Frascati, Italy
§Department of Physics, Faculty of Science, Osaka University, Tojonaka 560, Japan
@Dipartimento di Matematica e Fisica, Universita' di Camerino, 62032 Camerino, Italy

1. - INTRODUCTION

The intermediate valence of formally tetravalent compounds has been detected by XANES (X-ray Absorption Near Edge Structure) in CeO_2, PrO_2 and in TbO_2 but not in ThO_2 and UO_2 which have the same CaF_2 structure. These materials, in the framework of many body theoretical description of the ground state by the filled-band Anderson impurity model, can be classified as interatomic intermediate valence (IIV) systems whose specific properties are: i) a large mixing of 4f localized states with ligand valence orbitals, ii) a charge transfer energy δE (which determines the gap) smaller than the correlation energy U_{ff} ($U_{ff}>\delta E$) and iii) a hybridization energy V between 4f and oxygen 2p orbitals of the same order of magnitude as the energy separation ΔE between many body configuration $4f^n$ and $4f^{n+1}\underline{L}$, where $\underline{L}$ denotes a ligand hole ($V\sim\Delta E$).

Permanent address:
*Department of Physics, University of Rajasthn, Jaipur, INDIA
• Departamento de Fisica de la Materia Condensata, Universidad de Zaragoza, Zaragoza, SPAIN

Here we report the results of an extensive investigation of these materials by L_1-XANES, L_3-XANES and 3d XPS (x-ray photoemission spectroscopy) and we discuss the different many body final states probed by each spectroscopy.

The Ce L_3-XANES spectrum of CeO_2 has remained an unsolved puzzle for many years[1-5]. In fact the L_3-XANES spectra of actinides and lanthanides exhibit a single white line at threshold which is due to a resonance in the 2p->5d atomic cross section modified by local density of unoccupied states. This resonance can be obtained by one-electron theories[6] both using multiple scattering approach of XANES in the real space[7] as well as in the k space in the frame of band structure approach.[8]

The spectrum of CeO_2 on the other hand, shows two white lines like the spectra of mixed valent Ce intermetallics. Here we show that like in CeO_2, PrO_2 and TbO_2 L_3-XANES also show two white lines while ThO_2 and UO_2 show the one-electron spectra at M_3 edge. We interpret the white line of L_3-edge spectra by a many body calculation of the oscillator strength of the core 2p->5d excitations. The theory of the configuration interaction of the ground state of insulating oxides is required to obtain the many body final state. In CeO_2 by comparing the L_3-XANES and the 3d-XPS spectra we observe the key role played by the Coulomb interaction U_{df}=5 eV between the 5d photoelectron and the 4f electron.

The L_1-XANES of correlated rare earth dioxides show many body features beyond the one-electron description of photoabsorption calculated by full multiple scattering schema (FMS).[9,10]

2. - EXPERIMENTAL

The absorption experiment has been performed at the Frascati synchrotron radiation facility using the 1.5 Gev ADONE storage ring. Well characterized stochiometric samples were prepared by L. Albert and P. E. Caro at Laboratoire des Elements de Transition dans les Solids in Meudon (France).

XPS spectra have been measured by using a hemispherical electron analyser and the Al K_α-x ray emission line. Experimental details have been described elsewhere.[11,12]

3. - RESULTS AND DISCUSSION

In Fig.1 we report the L_1-XANES spectra of TbO_2, PrO_2 and CeO_2. The absorption coefficient has been normalized to the level of the atomic absorption jump at energies above the absorption edge. The zero of the energy scale has been fixed before the first weak absorption feature α.

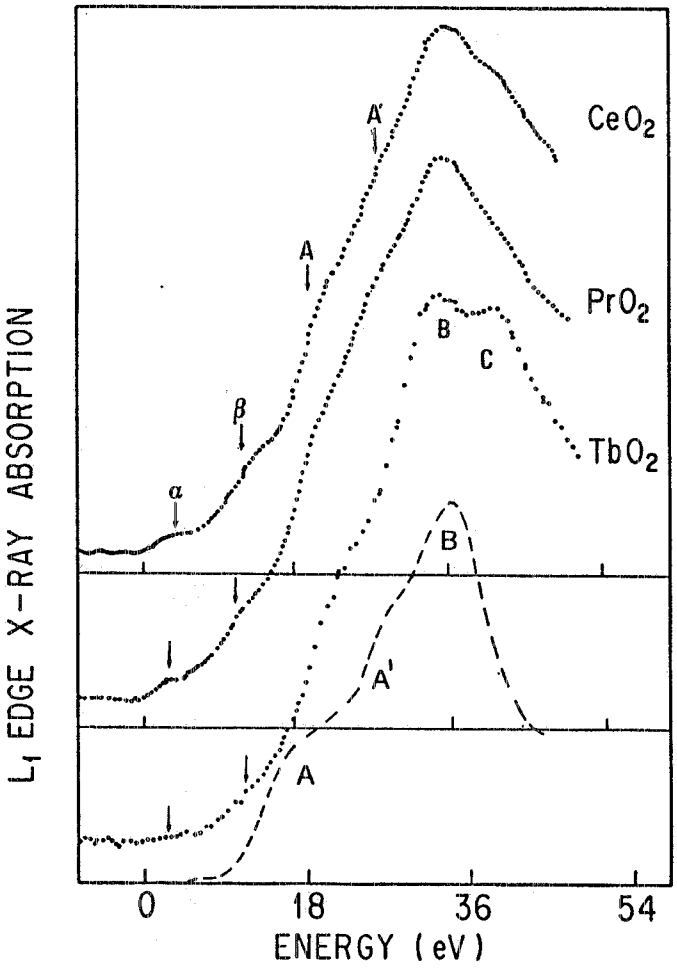

FIG. 1 - L_1 XANES of rare earth metal Ce, Pr and Tb of formally tetravalent oxides CeO_2, PrO_2 and TbO_2. The dashed curve in the lower part of the figure is the one-electron full multiple scattering XANES calculation, with 2 eV of broadening, of CeO_2 from transition from core 2s-level to p-final states for a cluster of six shells around cerium absorbing atom.

The dashed curve reported in the lower part of the figure is an "ab initio" full multiple scattering (FMS) calculation of the L_1-edge of cerium, including six shells around the absorbing cerium atom. Due to the lack of atomic resonances at the threshold of the 2s->6p transition the spectral features are due to multiple scattering resonances of the excited photoelectron within the cluster. Qualitative comparison of this one-electron calculation with the experimental results shows the presence of the one-electron structure A and B in all spectra. TbO_2, PrO_2 and CeO_2 have the same crystal structure and therefore we expect similar one-electron feature of unoccupied p states[13,14]. The presence of the weak features α, β and C are assigned to many body final states not predicted by one-electron XANES theory.

In Fig. 2 we show the $3d_{5/2}$ XPS spectra of CeO_2, PrO_2 and TbO_2. The spectra have been aligned to $\underline{3d}4f^n$ configuration, and the energy scale gives the energy separation of different satellites from the main line. The satellite peaks B and C which appear in CeO_2, have been interpreted by many body theories describing configuration interaction in the ground states[15-18]. In the spectrum of CeO_2 we observe no features induced by Ce^{3+} impurities, which often appear in the Ce 3d-XPS spectra between the B and C peaks. This is an experimental evidence that in the samples there are no reduced cerium atoms. TbO_2 shows a single intense satellite separated by 11eV which we assign to $\underline{3d}4f^8\underline{L}$ final state configuration, where $\underline{L}$ denotes a ligand hole.

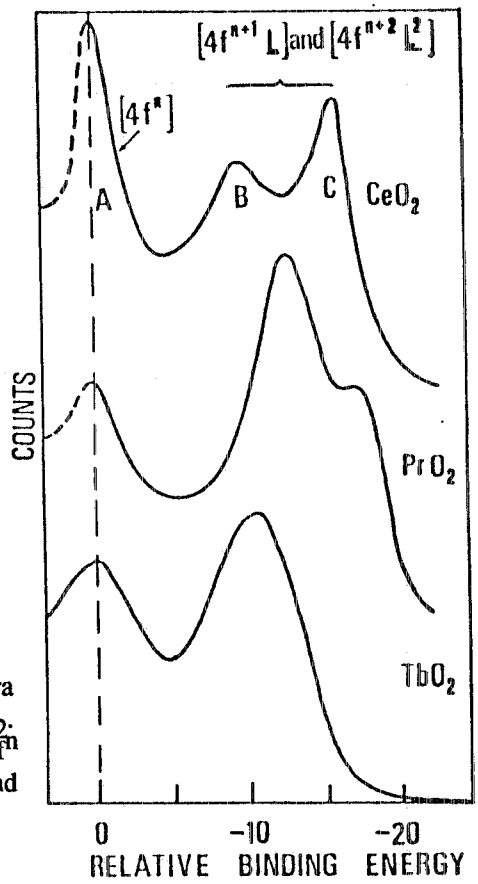

FIG. 2 - We report the $3d_{5/2}$ XPS spectra of Ce, Pr and Tb in CeO_2, PrO_2 and TbO_2. The spectra are aligned at the energy of $\underline{3d}4f^n$ configurations ($\underline{3d}4f^0$ for Ce, $\underline{3d}4f^1$ for Pr and $\underline{3d}4f^7$ for Tb).

In Fig. 3 we report the L_3-XANES spectra of CeO_2, PrO_2 and TbO_2. The U and Th M_3-XANES in UO_2 and ThO_2 in Fig.4 show at threshold a single white line due to a core transition to the unoccupied 6d orbitals enhanced by the resonance in the atomic absorption cross section for 3p->6d transitions.

The presence of two white lines in CeO_2, PrO_2 and TbO_2 shows the breakdown of the one-electron description for core transition in these systems. The different peaks correspond to different final state configurations with different configurations of valence electrons.

The electronic structure of correlated insulating IIV systems where there is a large mixing between localized 4f levels and more delocalized ligand (O 2p in our case) levels can be described by mixing of localized ionic multi-electron configurations: $4f^n$ and $4f^{n+1}\underline{L}$.

The ground state is described by the wavefunction

$$\Psi_g = a\,|\,4f^n\rangle + b\,|\,4f^{n+1}\underline{L}\rangle$$

The two ionic configurations before hybridization are separated by ΔE. The hybridization energy V between the atomic-like localized 4f and delocalized O 2p states determines the mixing between the multielectron configurations. In the final states at the white line of L_3 XANES for IIV systems the core hole is in the metal atom and the photoelectron is excited to the first 5d unoccupied band. The final state energies are determined by the Coulomb interaction Q_{hd} between the 5d electron and the core-hole, Q_{hf} between the f electrons and the core-hole and the Coulomb repulsion U_{df} between the 5d and the f electrons.

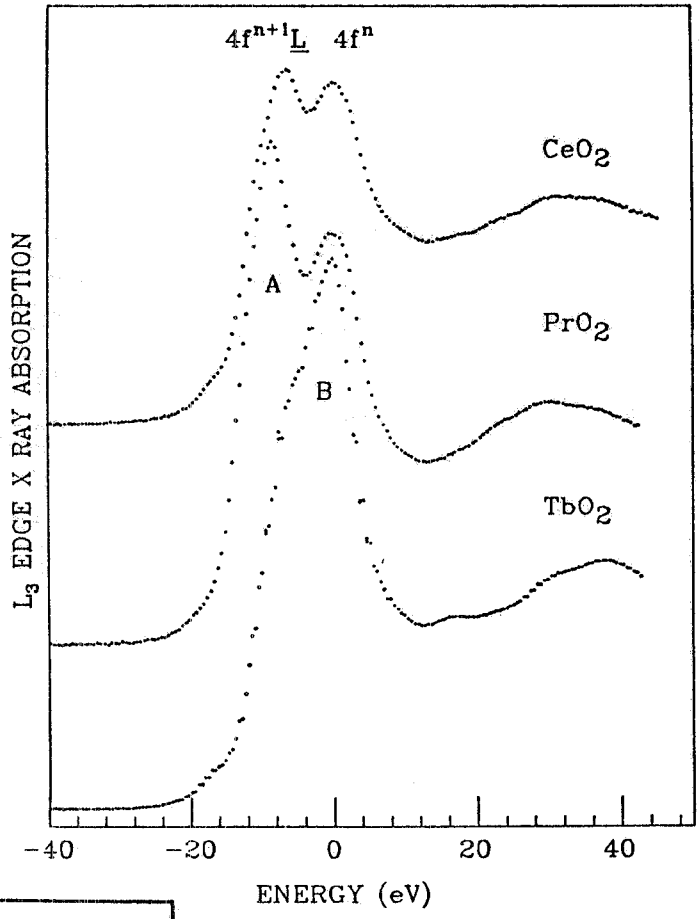

FIG. 3 - XANES spectra of CeO_2, PrO_2 and TbO_2 at metal L_3 threshold. The spectra have been aligned to $4f^n$ final state configurations.

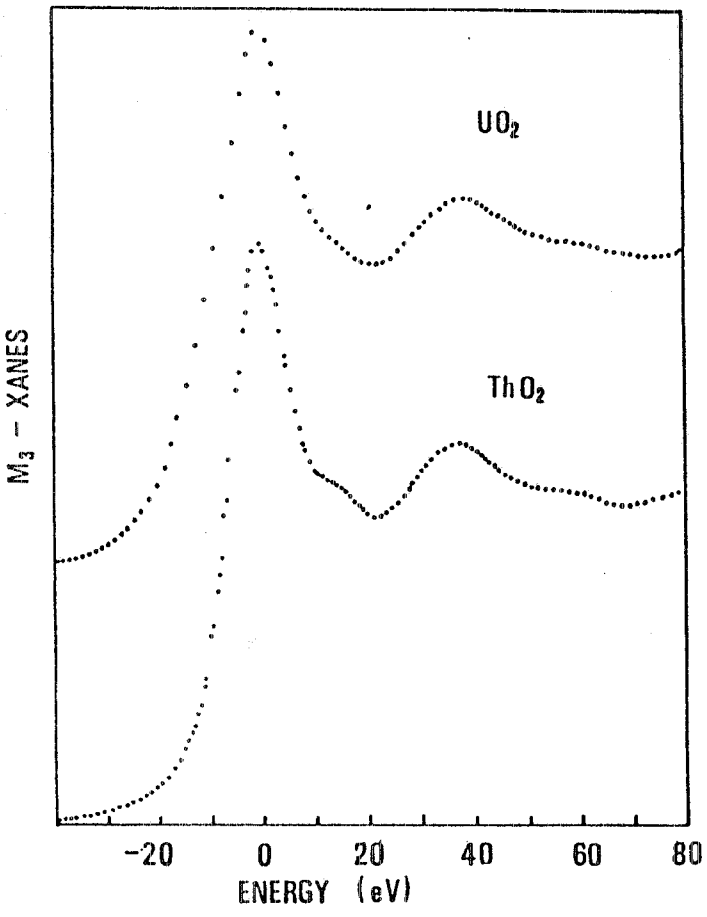

FIG.4 - M_3-XANES spectra of Th and U in formally tetravalent oxides with CaF_2 structure: ThO_2 and UO_2. The zero of the energy scale has been fixed to the maximum of both white lines.

As first pointed out by Kotani and Toyozawa[19] because of the large Q_{hf} interaction the f states are deepen by the core-hole in the XPS core final states. The L_3-XANES final states are different from XPS because the Coulomb repulsion U_{df} pushes up the f levels giving a reduced effective relaxation energy $Q_{hf}+ U_{df}$[5,19,20].

The fact that each core spectroscopy gives different final states with different energy separation and mixing of final state configurations is clearly shown by comparing Fig. 2 and Fig. 3.

The final states of IIV systems can be calculated using the filled band impurity Anderson model[17,20,21]. Within the cluster model a 4f level, a single (N=1) O 2p orbital with a mixing parameter V between them, and a single unoccupied 5d orbital are considered. The eigenstate, with the lowest energy E_g which is assumed to be a singlet state, of the initial state Hamiltonian is denoted by $|g\rangle$ and the L_3 absorption final state at energy E_f by $|f\rangle$. The calculations have been performed for the case of CeO_2. The band structure effects determine an oxygen 2p bandwith in MO_2 tetravalent oxides W=3eV.[13,14,22,23] To take account of this effect in the calculations we treat the valence band with energy ε^v_k as a finite system consisting of N discrete levels given by

$$\varepsilon^v_k=-W/2+W/N(k-1/2) \quad (k=1, \ldots . , N)$$

where N is the valence band width and we put W=3 eV; the center of the valence band is taken as the origin of energy. The Ce 5d band is similarly replaced by N discrete levels with the bandwidth 6 eV. Therefore the N=1 model is similar to the Fujimori cluster model and by increasing N we obtain the band structure model. The calculated $F_L(\omega)$ spectra for increasing values of N are found to converge for N>4 and Γ=1eV. The energy separation between the 4f level and the O 2p level (center of the O 2p valence band) is assumed to be δE=1.6 eV. The values of U_{ff} =10.5 eV and V=2.8 eV are obtained from analysis of 3d XPS core spectrum.[17,20] These values of δE, V and U_{ff} determine the interatomic intermediate valence in CeO_2 in the ground state giving non integer 4f count n_f=0.46.[17,21]

In the final state of L_3-XANES for the excitation of a 2p core hole and a 5d photoelectron we expect for CeO_2 three configurations $4f^0$, $4f^1$ and $4f^2$ separated approximately by:

$$E(f^1)<->E(f^0)= \delta E+Q_{hf}+U_{df}$$

$$E(f^2)<->E(f^0)=2(\delta E+Q_{hf}+U_{df}) +U_{ff}$$

We assign the many body features A and B of CeO_2 in Fig.3 to the $4f^1\underline{L}$ and $4f^o$ configurations respectively. The interaction Q_{hf} plays a key role in the final states of XPS spectra of 3d core lines. Q_{hd} and U_{df} are essential to describe the L_3-XANES final states. Here the value of Q_{hf}=-12.5 eV was determined from Ce(3d) XPS spectra as represented in ref. 17. The two quantities Q_{hd} and U_{df} were obtained as -6 eV and 5 eV, respectively, to reproduce the energy separation and relative

intensity of experimental peaks A and B in L_3 absorption spectra of CeO_2. The results of the many body calculations are plotted in Fig.5a for the cluster model N=1 and for the band model N=6. The energy separation between $4f^0$ and $4f^1\underline{L}$ configurations in the calculations is in good agreement with the energy separations of the white lines in CeO_2.

In Fig.5b we report the spectra of CeO_2 and cerium sulfate ($Ce(SO_4)_2+4H_2O$) which have similar cerium oxygen distance in the same site geometry. The large variation of intensities and lineshape of the peaks A and B appear clearly. Comparing the spectra of cerium sulfate we can see the effects due to different crystal structure for similar local structure. The sharpening of the A and B features in cerium sulfate is in qualitative agreement with the theoretical predictions shown in Fig.5a for the decreasing of the dispersion of the O 2p band going from CeO_2 to cerium sulfate.

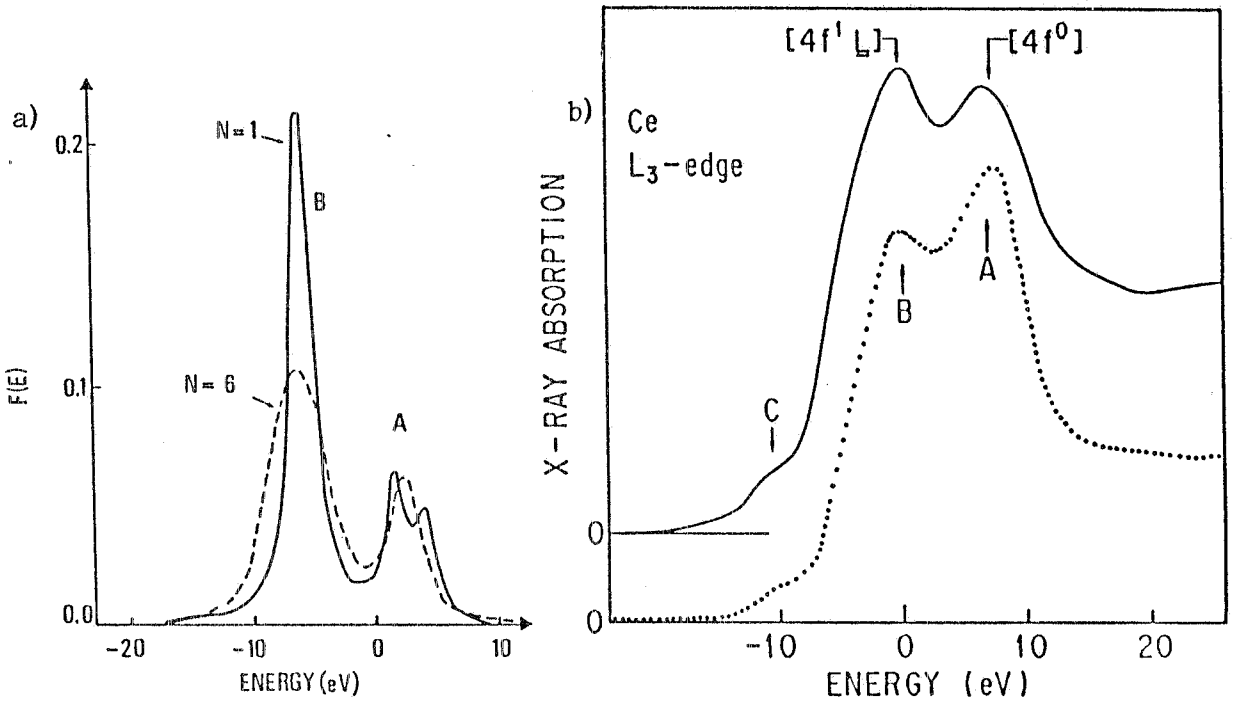

FIG.5 - **a)** Calculated core absorption spectra in the framework of filled band Anderson model for many body excitations with a 2p core hole and one electron in 5d states both in the limit of molecular cluster (N=1, solid lines) and in the limit of finite width (W=3eV) for filled valence and 5d bands (N=6, dashed lines). The theoretical parameters for calculation of the final states are U_{df}=5eV, Q_{hf}=-12.5eV and Q_{hd}=-6eV. The sharpening of the final states in the cluster limit is found.
b) L_3 absorption spectra of Ce in CeO_2 (solid lines) and $Ce(SO_4)_2+4H_2O$ (dotted line).

In the L_1-XANES spectra we have shown that the final state is determined by photoelectron multiple scattering resonances where the wavefunctions of the photoelectron is delocalized on a large cluster of about six shells around the photoabsorber. Therefore the Coulomb interaction between the p photoelectron in the continuum and the f electrons (U_{pf}) is expected to be smaller or negligible in comparison with U_{df} present in the atomic transition at the L_3 white lines. In fact the

L_1-XANES of Ce and Pr in CeO_2 and PrO_2 can be deconvoluted in three one-electron components with energy separation and intensity ratio as in 3d-XPS spectra. This shows that U_{pf} in L_1-XANES generally can be neglected. We are now working to obtain a description of the final state in L_1 and L_3-XANES and in core level XPS spectroscopy for each oxides, starting with the same parameters describing the many body configuration in the ground state.

4. - CONCLUSION

L_3-XANES and core level XPS are complementary methods for the determination of ground state properties of IIV systems. In fact in the final state of the 3d-XPS spectroscopy of CeO_2 we have a different situation because the $4f^{n+1}\underline{L}$ is mixed with the $4f^{n+2}\underline{L}^2$ configuration and well separated from $4f^n$ configuration.[17,24] On the contrary in L_3-XANES the $4f^{n+2}\underline{L}^2$ configuration in the final state is pushed at higher energy by U_{ff} and U_{df} contribution and therefore the low energy feature B is the mostly pure $4f^{n+1}\underline{L}$ configuration.

In conclusion the presence of the high binding energy line in XPS gives direct evidence of $4f^n$ configuration in the ground state while in L_3-XANES the low energy feature B gives a direct weight of the configuration $4f^{n+1}\underline{L}$ in the ground state. Therefore comparing the experimental results for CeO_2, PrO_2, TbO_2 and cerium sulfate we conclude that in these materials the probability of occupation of $4f^{n+1}\underline{L}$ configuration in the ground state is different from zero. Moreover the final state indicated by B in L_3-XANES for IIV material cannot be assigned to charge transfer final state shake-up satellites because it has been shown [5,11] that these satellites are strongly quenched in L_3 absorption.

REFERENCES

1. E. E. Vainsthein, S. Blokhin and Yu B. Paderno Sov. Phys. Solid State 6:2318 (1965).
2. G. Krill, J. P. Kappler, A. Meyer, L. Abadli and M. Ravet J.Phys. F 11:1713 (1981).
3. K. R. Bauchspiess, W. Boksch, E. Holland-Moritz, H. Launois, R. Pott and D. H. Wohlleben in:"Valence Fluctuations in Solids" eds. L. M. Falicov, W. Hanken and M. B. Maple, North Holland, Amsterdam New York, (1981) p.417.
4. A. Bianconi, M. Campagna and S. Stizza, Phys. Rev. B:25, 2477 (1982).
5. A. Bianconi, A. Marcelli, M. Tomellini and I. Davoli, J. Magnetism and Magnetic Materials 47&48:209 (1985).
6. A. Bianconi in: "X Ray Absorption: Principles, Applications and Techniques of EXAFS, SEXAFS and XANES" edited by R. Prinz and D. Konisberger, J. Wiley & Sons, New York (1985).
7. W. Kutzler, K. O. Hodgson, D. Misemer and S. Doniach, Chem. Phys. Lett. 92:626 (1982).
8. G. Materlik, J. E. Muller and J. W. Wilkins, Phys.Rev. Lett. 50:267 (1983).
9. A. Bianconi, M. Dell'Ariccia, P. J. Durham and J. B. Pendry, Phys. Rev. B 26:6502 (1982).
10. M. Benfatto, C. R. Natoli, A. Bianconi, J. Garcia, A. Marcelli, M. Fanfoni and I.Davoli Phys.Rev. B 34:5774 (1986).
11. A. Bianconi, A. Marcelli, I. Davoli, S. Stizza and M. Campagna, Solid State Commun. 49:409 (1984).
12. A. Bianconi, A. Kotani, T. Jo, K. Okada, R. Giorgi, A. Gargano, A. Marcelli and T. Miyahara, to be published.
13. D. D. Koelling, A. M. Boering and J. H. Wood, Solid State Commun. 47:227 (1983).
14. P. J. Kelly and M. S. S. Brooks, J. Phys. C 13: L939 (1980).
15. A. Fujimori, Phys.Rev. B 28:2281(1983); and Phys.Rev. B 28:4489(1983).
16. A. Fujimori, Phys.Rev. Lett. 53:2518 (1984).
17. A. Kotani, H. Mizuta, T. Jo and J. C. Parlebas Solid State Commun. 53:805 (1985); T. Jo and A. Kotani, J. Phys. Soc. Japan 55:2457 (1986).
18. A. Kotani and J. C. Parlebas, J. de Physique 46:77 (1985).
19. A. Kotani and Y. Toyozawa, J. Phys. Soc. Japan 35:1073 (1973); J. Phys.Soc. Japan 35:1082(1973) and J. Phys. Soc. Japan 37:912 (1974).
20. T. Jo and A. Kotani, Solid State Commun. 54:451 (1985)
21. A. Bianconi, A. Marcelli, H. Dexpert, R. Karnatak, A. Kotani, T. Jo and J. Petiau Phys.Rev. B 35:806 (1987).
22. E. Wuilloud, B. Delley, W. D. Schneider and Y. Baer, Phys. Rev. Lett. 53:202 (1984) and Phys. Rev. Lett. 53:2519 (1984).
23. Y. Baer and J. Schones, Solid State Commun. 54:451 (1985).
24. W.-D. Schneider, B. Delley, E. Wuilloud, J.-M. Imer and Y. Baer, Phys.Rev. B 32:6819 (1985).